Article

Six New Methyl Apiofuranosides from the Bark of *Phellodendron chinense* Schneid and Their Inhibitory Effects on Nitric Oxide Production

Peng-Fei Wang [1,2,†], Yan-Ping Li [1,2,†], Li-Qin Ding [2], Shi-Jie Cao [2], Li-Ning Wang [1,*] and Feng Qiu [1,2,*]

[1]   School of Chinese Materia Medica, Tianjin University of Traditional Chinese Medicine, Tianjin 300193, China; 13132166710@163.com (P.-F.W.); anney575@163.com (Y.-P.L.)
[2]   Tianjin State Key Laboratory of Modern Chinese Medicine, Tianjin University of Traditional Chinese Medicine, Tianjin 300193, China; ruby70303@163.com (L.-Q.D.); haojiejie_1988@126.com (S.-J.C.)
[*]   Correspondence: lining.wang@tjutcm.edu.cn (L.-N.W.); fengqiu20070118@163.com (F.Q.); Tel.: +86-22-5959-6238 (L.-N.W.); +86-22-5959-6223 (F.Q.)
[†]   These authors contributed equally to this work.

check for updates

Abstract: A chemical investigation on 70% EtOH extract from the bark of *Phellodendron chinense* Schneid (Rutaceae) led to six new methyl apiofuranosides (**1–6**), and ten known compounds (**7–16**). All these compounds were characterized by the basic analysis of the spectroscopic data including extensive 1D-, 2D-NMR (HSQC, HMBC), and high-resolution mass spectrometry, and the absolute configurations were determined by both empirical approaches and NOESY. Inhibitory effects of compounds **1–9** and **11–16** on nitric oxide production were investigated in lipopolysaccharide (LPS)-mediated RAW 264.7 cells, as a result, most of these isolates inhibited nitric oxide (NO) release, and among them **9, 11,** and **12** displayed the strongest inhibition on NO release at the concentration of 12.5 μM.

Keywords: *Phellodendron chinense* Schneid; methyl apiofuranoside; nitric oxide

1. Introduction

Phellodendron chinense Schneid is a deciduous tree also known as "Huang Bai" and found widely in the east and northeast of Asia [1]. The genus *Phellodendron*, belonging to the family Rutaceae, comprises of approximately 10 species. Among them, the bark of *P. chinense* Schneid, well-known as an oriental folk medicine, has been used for the treatment of meningitis, bacillary dysentery, pneumonia, tuberculosis, and liver cirrhosis for centuries, and is also an important natural source of berberine [2,3]. Previous phytochemical studies on this plant revealed the presence of alkaloids, which mainly belong to isoquinoline alkaloids, berberine-type, and aporphine-type [4]. In addition, some flavonoids, triterpenoids, and coumarins were also reported [5,6]. Pharmacology studies have demonstrated that its crude extracts and active compounds possess wide pharmacological activities, especially hypoglycemic, anti-inflammatory, and antibacterial activities [7,8]. The reports of methyl apiofuranosides are relatively rare [9,10]; during the course of our investigation on the chemical components of *P. chinense* Schneid, six new methyl apiofuranosides (**1–6**) (Figure 1) and ten phenolic acids (**7–16**) were obtained. In this report, their isolation, structural characterization, and inhibitory effects on nitric oxide production are described.
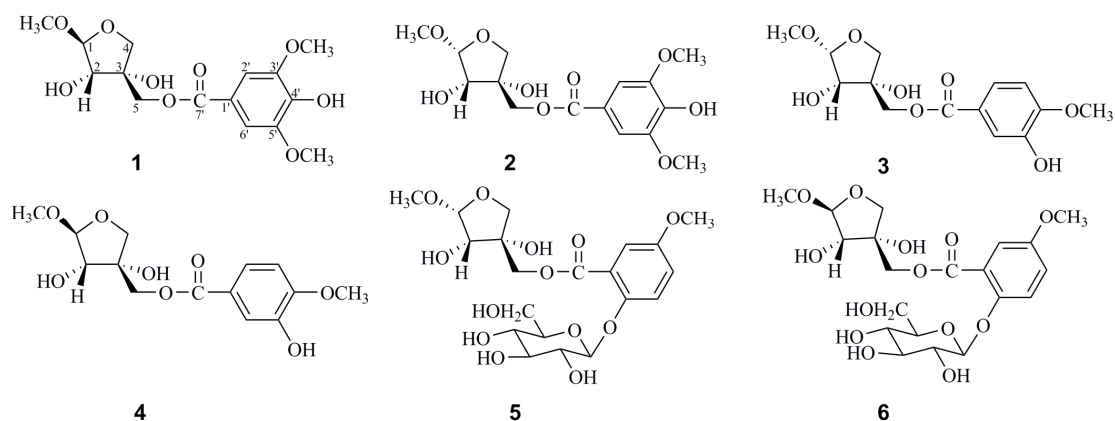
Figure 1. Structures of compounds **1–6**.

2. Results

Methyl 5-*O*-(4′-hydroxy-3′,5′-dimethoxy-benzoyl)-β-ᴅ-erythro-apiofuranoside (**1**), afforded a molecular formula of $C_{15}H_{20}O_9$ based on the (−)-high-resolution electrospray ionization mass spectra (HRESIMS) ion peak at *m/z* 343.1032 [M − H]⁻ (calcd for $C_{15}H_{19}O_9$, 343.1029), indicating six degrees of hydrogen deficiency. The characteristic IR absorptions demonstrated the presence of hydroxy (3412 cm⁻¹) and benzene ring (1621, 1112, and 615 cm⁻¹) groups. The ¹H-NMR spectrum of **1** exhibited typical signals for three methoxyl groups (δ_H 3.89, s, 3H; 3.89, s, 3H; 3.37, s, 3H) and one set of protons of the aromatic system (δ_H 7.35, 2H, s) (Table 1). In addition, signals in the region of δ_H 3.50–5.50 mainly came from one sugar unit, characterized by an anomeric proton signal at δ_H 4.86 (1H, d, *J* = 2.5 Hz). In the ¹³C-NMR spectrum, apart from six characteristic carbon signals for a benzene ring at δ_C 121.2, 108.5, 149.1, 142.3, 149.1, and 108.5, nine carbon resonances were observed and ascribed to one ester carbonyl at δ_C 167.9, five oxygen bearing carbons at δ_C 111.6, 78.9, 79.1, 75.0, and 67.7 and three methoxy carbons at δ_C 57.0, 57.0, and 56.0 with the aid of an HSQC experiment. These characteristic signals, in combination with the HRESIMS data, implied that **1** is a methyl apiofuranose [11]. According to previous reports, apiose unit with 1-OH and 2-OH in trans configuration presents constant coupling $J_{1,2}$ 0–2 Hz, whereas cis configuration is characterized by $J_{1,2}$ 3–4 Hz [12,13]. It should be noted that there was no apiose authentic sample at hand, and this branched chain sugar can occur in four isomeric forms. The β-ᴅ-apiofuranose moiety was characterized on the basis of the carbon chemical shift and the coupling constant of the anomeric proton, in combination with the NOE correlation between H-2 and H-5 [9,14–16]. The methyl apiose unit was therefore identified as a methyl β-ᴅ-apiofuranoside based on the anomeric proton singlet at δ_H 4.86 (1H, d, *J* = 2.5 Hz), the chemical shift of C-1 at 111.6, and on the NOESY correlation between H-2 (δ_H 3.97, d, *J* = 2.5 Hz) and H-5 (δ_H 4.32, s, 2H) by empirical approaches reported by Ishii [9]. Furthermore, the observable HMBC correlations (Figure 2) of 3′-OCH₃/C-3′; 5′-OCH₃/C-5′; H-2′ and H-6′/C-7′; 1-OCH₃/C-1 were used to establish 4′-hydroxy-3′,5′-dimethoxy-benzoyl. HMBC correlations from H-5 (δ_H 4.32) to the ester carbonyl at δ_C 167.9 (C=O) suggested that the benzoyl group was attached to C-5 of the methyl apiose unit (Figures S1-1–S1-9). Consequently, the structure of **1** was determined to be methyl 5-*O*-(4′-hydroxy-3′,5′-dimethoxy-benzoyl)-β-ᴅ-erythro-apiofuranoside, and elucidated as shown in Figure 1.

Table 1. ^{1}H-NMR (600 MHz) and ^{13}C-NMR (150 MHz) spectroscopic data for compounds **1–4**.

Position	1 [a]		2 [a]		3 [a]		4 [a]	
	δ_C	δ_H (*J* in Hz)	δ_C	δ_H (*J* in Hz)	δ_C	δ_H (*J* in Hz)	δ_C	δ_H (*J* in Hz)
Api-1	111.6	4.86 (1H, d, *J* = 2.5 Hz)	104.7	4.90 (1H, d, *J* = 4.6 Hz)	104.7	4.90 (1H, d, *J* = 4.6 Hz)	111.6	4.86 (1H, d, *J* = 2.6 Hz)
2	78.9	3.97 (1H, d, *J* = 2.5 Hz)	74.5	3.99 (1H, d, *J* = 4.6 Hz)	74.4	3.99 (1H, d, *J* = 4.6 Hz)	78.8	3.96 (1H, d, *J* = 2.6 Hz)
3	79.1		76.6		76.7		79.1	
4	75.0	4.04 (1H, d, *J* = 9.8 Hz) 3.89 (1H, d, *J* = 9.8 Hz)	75.4	4.07 (1H, d, *J* = 9.9 Hz) 3.91 (1H, d, *J* = 9.9 Hz)	75.4	4.07 (1H, d, *J* = 9.8 Hz) 3.91 (1H, d, *J* = 9.8 Hz)	75.0	4.03 (1H, d, *J* = 9.8 Hz) 3.89 (1H, d, *J* = 9.8 Hz)
5	67.7	4.32 (2H, m)	68.7	4.29 (2H, m)	68.4	4.28 (2H, m)	67.5	4.31 (2H, m)
1'	121.2		121.2		125.4		125.4	
2'	108.5	7.35 (1H, s)	108.5	7.35 (1H, s)	116.1	7.59 (1H, d, *J* = 1.9 Hz)	116.1	7.59 (1H, d, *J* = 1.9 Hz)
3'	149.1		149.1		148.9		148.9	
4'	142.3		142.3		153.2		153.2	
5'	149.1		149.1		113.9	6.84 (1H, d, *J* = 8.8 Hz)	113.8	6.85 (1H, d, *J* = 8.0 Hz)
6'	108.5	7.35 (1H, s)	108.5	7.35 (1H, s)	122.4	7.57 (1H, dd, *J* = 8.8, 1.9 Hz)	122.4	7.58 (1H, dd, *J* = 8.0, 1.9 Hz)
7'	167.9		167.9		168.0		168.0	
3'-OCH$_3$	57.0	3.89 (3H, s)	57.0	3.88 (3H, s)				
4'-OCH$_3$					56.6	3.90 (3H, s)	56.6	3.90 (3H, s)
5'-OCH$_3$	57.0	3.89 (3H, s)	57.0	3.88 (3H, s)				
1-OCH$_3$	56.0	3.37 (3H, s)	56.0	3.43 (3H, s)	55.7	3.43 (3H, s)	55.7	3.38 (3H, s)

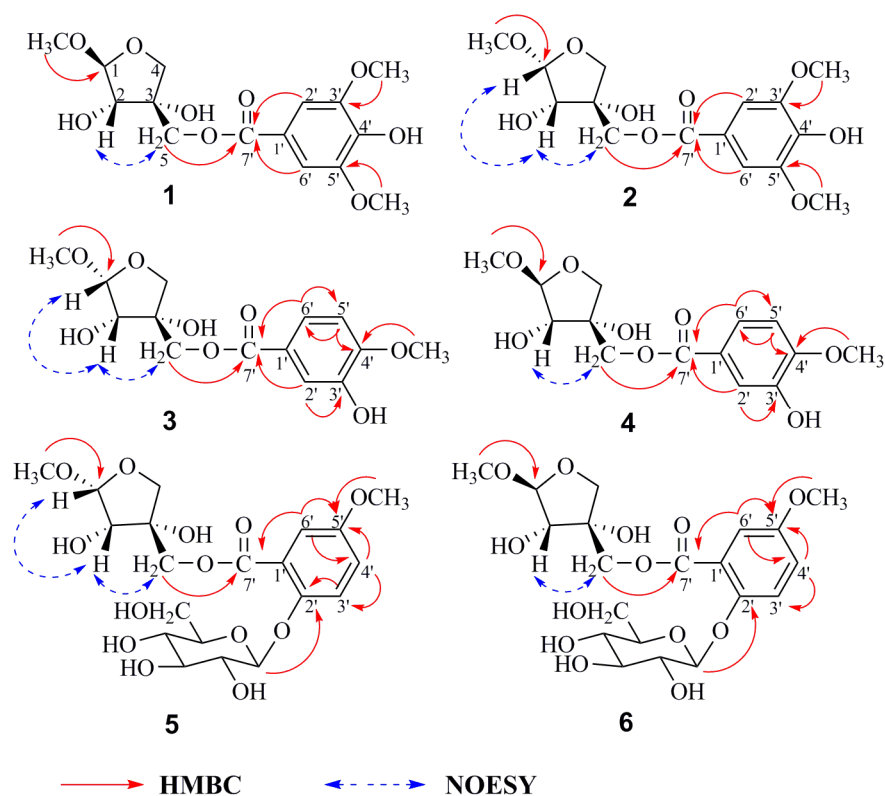[a] Data were recorded in CD$_3$OD.

Figure 2. Key HMBC and NOESY correlations of compounds **1**–**6**.

The same molecular formula, $C_{15}H_{20}O_9$, for **2** (methyl 5-*O*-(4′-hydroxy-3′,5′-dimethoxy-benzoyl)-α-D-erythro-apiofuranoside) was established based on its (−)-HRESIMS ion peak at *m/z* 343.1031 (calcd for $C_{15}H_{19}O_9$, 343.1029). Analysis of the NMR spectroscopic data suggests that **2** shares the same methyl apiofuranoside skeleton as **1**, except for two differences in the chemical shift of C-1 and $J_{1,2}$. Their respective chemical shift of C-1 exhibited 104.7 in **2** but 111.6 in **1**, furthermore, $J_{1,2}$ = 4.6 Hz in **2** and $J_{1,2}$ = 2.5 Hz in **1** (Table 1). The methyl apiose unit was therefore identified as a methyl α-D-apiofuranoside based on the anomeric proton singlet at δ_H 4.90 (1H, d, *J* = 4.6 Hz), the chemical shift of C-1 at δ_C 104.7, and on the NOESY correlation among H-2 (δ_H 3.99, d, *J* = 4.6 Hz), H-5 (δ_H 4.29, m, 2H), and H-1 (δ_H 4.90, d, *J* = 4.6 Hz) [14]. In comparison of the NOESY spectrum of **2** and **1**, there are correlations between H-2/H-1 and H-5/H-1 in **2**, while H-2/H-5 has the correlation in **1** only (Figures S2-1–S2-9). The structure of compound **2** was proposed as shown.

Methyl 5-*O*-(2′-hydroxyl-5′-methoxyl-benzoyl)-α-D-erythro-apiofuranoside (**3**), afforded a molecular formula of $C_{14}H_{18}O_8$ based on the (−)-HRESIMS ion peak at *m/z* 313.0921 [M − H]⁻ (calcd for $C_{14}H_{17}O_8$, 313.0923), corresponding to six degrees of hydrogen deficiency. The characteristic IR absorptions demonstrated the presence of hydroxy (3415 cm^{-1}) and benzene ring (1604 and 1458 cm^{-1}) groups. The ^{1}H-NMR spectrum indicated that compound **3** had two methoxyl groups (δ_H 3.90, s, 3H and 3.43, s, 3H) and one set of protons of the aromatic system at δ_H 7.59 (1H, d, *J* = 1.9 Hz, H-2′), 7.57 (1H, dd, *J* = 8.8, 1.9 Hz, H-6′) and 6.84 (1H, d, *J* = 8.8 Hz, H-5′), revealing three aromatic protons coupled in an ABX pattern. Analysis of ^{1}H-NMR and ^{13}C-NMR spectroscopic data suggests that **3** shares the same methyl apiofuranose-type skeleton as **2** (Figures S3-1–S3-9, Supporting Information). In addition, the observable HMBC correlations (Figure 2) of 3′-OCH₃/C-3′; H-5′/C-4′ and C-6′; H-6′/C-5′ and C-7′; and H-2′/C-3′ and C-7′ were used to establish the 2′-hydroxyl-5′-methoxyl-benzoyl moiety. The structure of compound **3** was assigned as shown.

The same molecular formula, $C_{14}H_{18}O_8$, for **4** was established based on its (−)-HRESIMS ion peak at *m/z* 313.0927 (calcd for $C_{14}H_{17}O_8$, 313.0923), respectively. Analysis of their NMR spectroscopic data suggests that **4** shares the same methyl apiofuranoside skeleton as **3**, except

for two differences in the chemical shift of C-1 and $J_{1,2}$. Their respective chemical shift of C-1 exhibited 111.6 in **4** and 104.7 in **3**, $J_{1,2}$ = 2.6 Hz in **4** and $J_{1,2}$ = 4.6 Hz in **3** (Table 1). In addition, NOESY data facilitated the determination of the absolute configuration of methyl 5-*O*-(3′-hydroxyl-4′-methoxyl-benzoyl)-β-ᴅ-erythro-apiofuranoside (Figures S4-1–S4-9).

Methyl 5-*O*-(2′-*O*-β-ᴅ-glucosyl-5′-methoxyl-benzoyl)-α-ᴅ-erythro-apiofuranoside (**5**) afforded a molecular formula of $C_{20}H_{28}O_{13}$ based on the HRESIMS ion peak at *m/z* 521.1513 [M + COOH]⁻ (calcd for $C_{21}H_{29}O_{15}$, 521.1506), corresponding to seven degrees of hydrogen deficiency. Its ¹H-NMR data revealed the signals for two methoxyl groups (δ_H 3.90, s, 3H; 3.43, s, 3H), one set of protons of the aromatic system at δ_H 7.64 (1H, d, *J* = 2.0 Hz, H-6′), 7.68 (1H, dd, *J* = 8.5, 2.0 Hz, H-4′) and 7.22 (1H, d, *J* = 8.5 Hz, H-3′) revealing three aromatic protons coupled in an ABX pattern, two sugar anomeric proton signals at δ_H 4.90 (1H, d, *J* = 4.5 Hz) and 5.03 (1H, d, *J* = 7.6 Hz) (Table 2). The ¹³C-NMR spectroscopic data suggests that the presence of an ester carbonyl, a benzene ring, a methyl apioforanose, a glucose and two methoxyl groups in **5**, with the aid of an HSQC experiment. The acid hydrolysis of **5** followed by derivatization with ʟ-cysteine methyl ester liberated ᴅ-glucose, which were identified by applying HPLC systems equipped with UV detectors and C_{18} reversed-phase columns [17,18]. In addition, the observable HMBC correlations (Figure 2) of H-1′′/C-2′; H-6′/C-4′, C-5′, C-7′; H-3′/C-2′, C-4′; H-4′/C-3′, C-5′; 5′-OCH₃/C-5′ and H-5/C-7′ were used to establish 2′-*O*-β-D-glucosyl-5′-methoxyl-benzoyl. Similarly, the configuration of **5** was deduced by the analysis of the NOESY spectrum (Figures S5-1–S5-9).

Table 2. ¹H-NMR (600 MHz) and ¹³C-NMR (150 MHz) spectroscopic data for compounds **5–6**.

	5 [a]		**6** [a]	
Position	δ_C	δ_H (*J* in Hz)	δ_C	δ_H (*J* in Hz)
Api-1	104.7	4.90 (1H, d, *J* = 4.5 Hz)	111.6	4.86 (1H, d, *J* = 2.6 Hz)
2	74.5	4.00 (1H, d, *J* = 4.5 Hz)	78.8	3.96 (1H, d, *J* = 2.6 Hz)
3	76.6		79.1	
4	75.4	4.07 (1H, d, *J* = 10.0 Hz) 3.92 (1H, d, *J* = 10.0 Hz)	75.0	4.03 (1H, d, *J* = 9.8 Hz) 3.90 (1H, d, *J* = 9.8 Hz)
5	68.7	4.31 (2H, m)	67.8	4.33 (2H, m)
1′	125.3		125.3	
2′	152.5		152.5	
3′	116.6	7.22 (1H, d, *J* = 8.5 Hz)	116.6	7.22 (1H, d, *J* = 8.5 Hz)
4′	124.9	7.68 (1H, dd, *J* = 8.5, 2.0 Hz)	124.9	7.67 (1H, dd, *J* = 8.5, 2.0 Hz)
5′	150.6		150.6	
6′	114.5	7.64 (1H, d, *J* = 2.0 Hz)	114.5	7.64 (1H, d, *J* = 2.0 Hz)
7′	167.6		167.5	
5′-OCH₃	56.9	3.90 (3H, s)	56.9	3.91 (3H, s)
1-OCH₃	55.7	3.43 (3H, s)	56.0	3.38 (3H, s)
Glc-1′′	102.1	5.03 (1H, d, *J* = 7.6 Hz)	102.1	5.03 (1H, d, *J* = 7.6 Hz)
2′′	74.9	3.53 (1H, m)	75.0	3.53 (1H, m)
3′′	78.6	3.47 (1H, m)	78.5	3.47 (1H, m)
4′′	71.4	3.40 (1H, m)	71.4	3.42 (1H, m)
5′′	78.0	3.49 (1H, m)	78.0	3.49 (1H, m)
6′′	62.6	3.70 (1H, dd, *J* = 12.0, 5.6 Hz) 3.87 (1H, m)	62.6	3.69 (1H, dd, *J* = 12.0, 5.6 Hz) 3.88 (1H, m)

[a] Data were recorded in CD₃OD.

The HRESIMS of **6** displayed an ion peak at *m/z* 521.1516 [M + COOH]⁻ (calcd for $C_{21}H_{29}O_{15}$, 521.1506), suggesting that this compound shares the same molecular formula ($C_{20}H_{28}O_{13}$) as that of **5**. The resonances in its NMR data (Figures S4-4–S4-7) demonstrated the planar structure of **4** was similar to that of **5** except for two differences in the chemical shift of C-1 and $J_{1,2}$. However, the NOESY correlations among H-2 (δ_H 3.96, d, *J* = 2.6 Hz) and H-5 (δ_H 4.33, m, 2H) were indicative of a β-ᴅ-erythro-apiofuranoside in **6**, which was opposite that of **5**, and further supported by the

^{1}H-NMR and downfield-shifted resonance of H-1 at δ_H 4.86 (1H, d, *J* = 2.6 Hz) and chemical shift of C-1 exhibited 111.6 in ^{13}C-NMR (Figures S6-1–S6-9). The structure of compound **6** (methyl 5-*O*-(2′-*O*-β-ᴅ-glucosyl-5′-methoxyl-benzoyl)-β-ᴅ-erythro-apiofuranoside) was proposed as shown.

Ten known compounds were identified as *p*-coumaric acid (**7**) [19], trans-ferulic acid (**8**) [20], 3,4-dimethoxycinnamic acid (**9**) [21], methyl-*p*-coumarate (**10**) [22], caffeic acid methyl ester (**11**) [23], ferulic acid methyl ester (**12**) [24], (−)-5-*O*-feruloylquinic acid methyl ester (**13**) [25], methyl 4-hydroxybenzoate (**14**) [26], ethyl 3,4-dihydroxybenzoate (**15**) [27], and 4-hydroxy-3,5-dimethoxy benzoic acid methyl ester (**16**) [28] based on their obtained spectroscopic data.

Nitric oxide (NO) is a diatomic free radical that is extremely short lived in biological systems. It is generated from ʟ-arginine by nitric oxide synthase (NOS) and plays an important role in the regulation of physiological responses. The generation of NO is closely associated with inflammation, tumors, and immunoregulation [29–31]. In this study, all compounds isolated from the bark of *P. chinense* Schneid were examined for their inhibitory effects on NO production induced by lipopolysaccharide (LPS) in RAW 264.7 cells. In order to exclude the inhibition of NO production caused by cell cytotoxicity, cell viability was evaluated by the MTT method [32]. RAW 264.7 cell was treated with various concentrations of isolates for 24 h and the cell viability was tested by MTT assay as described in Section 2. As shown in Figure 3, the results revealed that no obvious cytotoxicity (over 85% cell survival) for most of compounds at the concentrations range of 6.25–100 μM was observed except for compound **10**. Thus, the NO levels were detected in the RAW 264.7 cells after treated with 12.5 μM, 25 μM, and 50 μM of the tested compounds in subsequent experiments. Most of the isolated compounds inhibited NO release, as shown in Figure 4, and among them methyl apiofuranosides **1**, **4,** and **6** exhibited the inhibition on NO release at the concentration of 12.5 μM, while **2**, **3,** and **5** did not affect NO production. Meanwhile, compounds **9**, **11,** and **12** displayed the strongest inhibition on NO release, compared with the positive control berberine [33]. Together, three new methyl apiofuranosides including **1**, **4**, and **6** need to be further investigated on the pharmacological properties of NO inhibition.
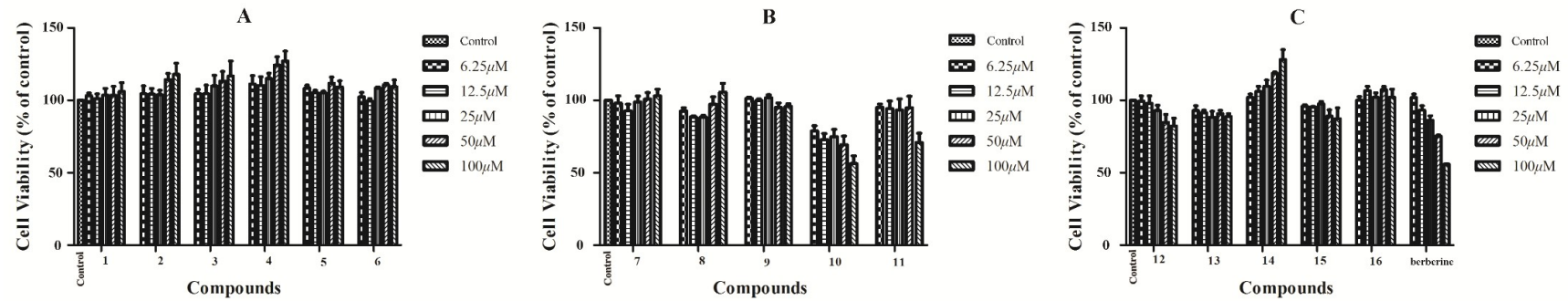
Figure 3. Effects of compounds 1–6 (**A**), compounds 7–11 (**B**), compounds 12–16 and Berberine (**C**) on RAW 246.7 cell viability (6.25–100 μM) compared to the control group (without compound group). Data are represented as mean ± SD of three independent experiments.
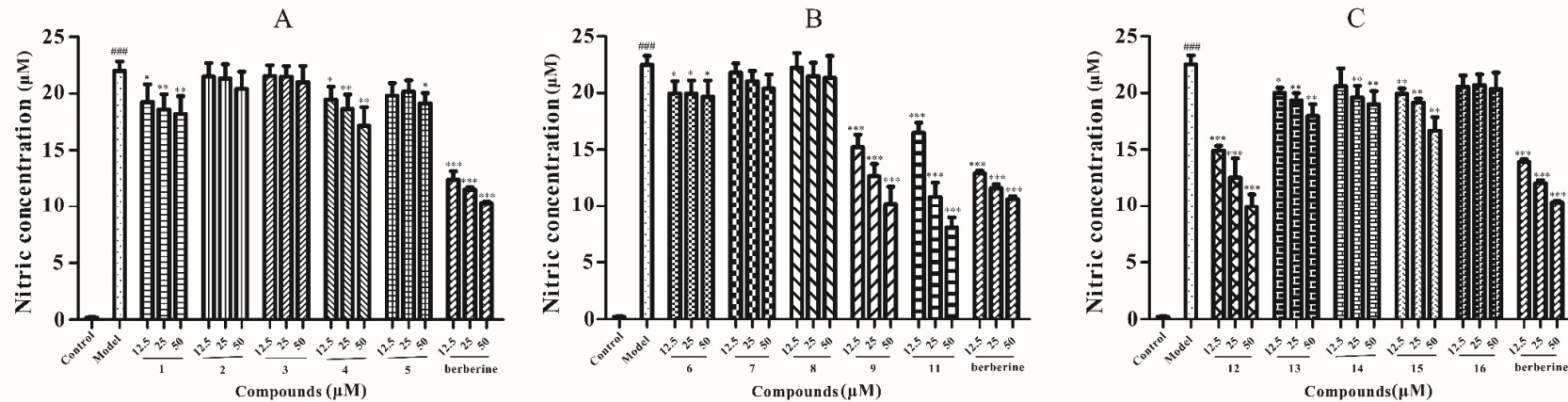

Figure 4. Nitric oxide (NO) inhibitory activity of compounds 1–5 (**A**), compounds 6–9, 11 (**B**) and compounds 12–16 (**C**) on RAW 264.7 cell (12.5 μM, 25 μM, 50 μM). $^{###}$ $p < 0.001$, compared to the control group (without lipopolysaccharide (LPS)-treated group); * $p < 0.05$, ** $p < 0.01$, and *** $p < 0.001$ compared to the model group (with LPS-treated group). Data are represented as mean ± SD of three independent experiments.

3. Materials and Methods

3.1. General Experimental Procedure

Optical rotations were measured with a AUTOPOL IV polarimeter (Rudolph, Hackettstown, NJ, USA). The UV spectra were determined by a UV-2450 visible spectrophotometer (Shimadzu, Tokyo, Japan). Infrared spectra were collected using KBr disks on a Tensor 27 infrared spectrometer (Bruker Beijing Scientific Tech Co., Beijing, China). NMR spectra were recorded on a Bruker ARX-600 spectrometer (600 MHz for ^{1}H and 150 MHz for ^{13}C, Bruker Beijing Scientific Tech Co., Beijing, China) in CD_3OD with tetramethylsilane as an internal standard. Chemical shifts were expressed in δ (ppm), and coupling constants (J) were reported in Hz. High-resolution electrospray ionization mass spectra (HRESIMS) were acquired on a Waters Xevo G2-S UPLC-Q/TOF mass spectrometer (Water, Milford, MA, USA). Preparative HPLC was performed with an ODS column (C-18, 250 × 20 mm, Inertsil Pak, Tokyo, Japan) in a Waters 600 liquid chromatograph apparatus equipped with a Waters 490 UV detector (Water, Milford, MA, USA). Methanol was HPLC grade. Sigel 60 (Qingdao Haiyang Chemical Co., Ltd., Qingdao, China), Sephadex LH-20 (Advanced Technology Industrial Co., Ltd., Hongkong, China), and ODS (40–75 μm, FujiSilysia Chemical Ltd., Kyoto, Japan) were used as column chromatography stationary phases. TLC was carried out on a silica gel 60 plate 20 × 20 cm (Merck, Berlin, Germany). RP-HPLC was performed on an Agilent 1260 Series instrument with an RP-C_{18} column (20 × 200 mm i.d., Shim-pack, Shimadzu, Tokyo, Japan).

3.2. Plant Material

The dried bark of *P. chinense* Schneid was collected in Anguo, Hebei Province, People's Republic of China. A voucher specimen (AP-2014-62) was identified by Professor Li-Juan Zhang and deposited at the School of Chinese Materia Medica, Tianjin University of Traditional Chinese Medicine.

3.3. Extraction and Isolation

The plant material (9.0 kg) was cut into small pieces and heated at reflux with 70% aqueous EtOH (3 × 90 L). The resulting EtOH extract was concentrated in vacuo at 40 °C, suspended in H_2O (5 L). A total of 4% dilute sulfuric acid adjusted the pH to 4–5, followed by enrichment of alkaloids by 732 cation-exchange resins to obtain alkaloid fraction (20 g) and non-alkaloid fraction (435 g). The non-alkaloids were detected by TLC, and the Dragendorff's reagent reaction was negative. The non-alkaloid fraction (435 g) was first fractionated by macroporous adsorptive resin D101, eluted with a step gradient system of EtOH/H_2O (*v/v*, 0–100%), to afford six subfractions (N1–N6). The N5 (32 g) was subjected to silica gel column chromatography (10 cm × 120 cm) using a gradient mixture of CH_2Cl_2-MeOH (100:0, 100:1, 70:1, 50:1, 30:1, 10:1, 5:1, 1:1, 0:100) as eluent to give eight fractions (N51–N58). N51 was eluted with CH_2Cl_2-MeOH (1:1) on Sephadex LH-20 and then further purified by ODS column chromatography eluted with MeOH/H_2O (20:80, 50:50, 80:20) and by repeated RP-18 HPLC preparation to give **1** (11.0 mg), **2** (22.0 mg), **3** (10.6 mg), **4** (8.6 mg), **5** (9.6 mg), and **6** (10.4 mg).

Methyl 5-O-(4'-hydroxy-3',5'-dimethoxy-benzoyl)-β-ᴅ-erythro-apiofuranoside (**1**): colorless or white acicular crystal; $[\alpha]_D^{25}$ −24° (*c* 0.1, MeOH); UV (MeOH) λ_{max} (log ε) 216 (4.3), 279 (4.0) nm; IR (KBr) ν_{max} 3412, 2968, 1621, 1112, 1054, 1024, 615 cm^{-1}; ^{1}H and ^{13}C-NMR data (Table 1); HRESIMS *m/z* 343.1032 [M − H]$^−$ (calcd for $C_{15}H_{19}O_9$, 343.1029).

Methyl 5-O-(4'-hydroxy-3',5'-dimethoxy-benzoyl)-α-ᴅ-erythro-apiofuranoside (**2**): colorless oil; $[\alpha]_D^{25}$ +50° (*c* 0.1, MeOH); UV (MeOH) λ_{max} (log ε) 217 (4.3), 279 (4.0) nm; IR (KBr) ν_{max} 3416, 2965, 1619, 1463, 1363, 1222, 1045, 778, 612 cm^{-1}; ^{1}H and ^{13}C-NMR data (Table 1); HRESIMS *m/z* 343.1031 [M − H]$^−$ (calcd for $C_{15}H_{19}O_9$, 343.1029).

Methyl 5-O-(2'-hydroxyl-5'-methoxyl-benzoyl)-α-ᴅ-erythro-apiofuranoside (**3**): colorless oil; $[\alpha]_D^{25}$ +56° (*c* 0.1, MeOH); UV (MeOH) λ_{max} (log ε) 204 (4.0), 264 (3.8) nm; IR (KBr) ν_{max} 3415, 2941, 1707, 1604, 1275,

1059, 768 cm^{-1}; ^{1}H and ^{13}C-NMR data (Table 1); HRESIMS *m/z* 313.0921 [M − H]$^-$ (calcd for C$_{14}$H$_{17}$O$_8$, 313.0923).

Methyl 5-O-(3′-hydroxyl-4′-methoxyl-benzoyl)-β-ᴅ-erythro-apiofuranoside (**4**): colorless oil; [α]$_D^{25}$−6° (*c* 0.1, MeOH); UV (MeOH) λ$_{max}$ (log ε) 204 (4.0), 264 (3.8) nm; IR (KBr) ν$_{max}$ 3414, 2938, 2351, 1717, 1522, 1467, 1324, 1048, 616 cm^{-1}; ^{1}H and ^{13}C-NMR data (Table 1); HRESIMS *m/z* 313.0927 [M − H]$^-$ (calcd for C$_{14}$H$_{17}$O$_8$, 313.0923).

Methyl 5-O-(2′-O-β-ᴅ-glucosyl-5′-methoxyl-benzoyl)-α-ᴅ-erythro-apiofuranoside (**5**): colorless oil; [α]$_D^{25}$+14° (*c* 0.1, MeOH); UV (MeOH) λ$_{max}$ (log ε) 204 (4.2), 257 (3.8) nm; IR (KBr) ν$_{max}$ 2947, 2351, 1518, 1463, 1375, 1321, 1025, 668 cm^{-1}; ^{1}H and ^{13}C-NMR data (Table 2); HRESIMS *m/z* 521.1513 [M + COOH]$^-$ (calcd for C$_{21}$H$_{29}$O$_{15}$, 521.1506).

Methyl 5-O-(2′-O-β-ᴅ-glucosyl-5′-methoxyl-benzoyl)-β-ᴅ-erythro-apiofuranoside (**6**): colorless oil; [α]$_D^{25}$−24° (*c* 0.1, MeOH); UV (MeOH) λ$_{max}$ (log ε) 204 (4.2), 257 (3.8) nm; IR (KBr) ν$_{max}$ 2962, 2351, 1701, 1522, 1467, 1048, 669 cm^{-1}; ^{1}H and ^{13}C-NMR data (Table 2); HRESIMS *m/z* 521.1516 [M + COOH]$^-$ (calcd for C$_{21}$H$_{29}$O$_{15}$, 521.1506).

3.4. Sugar Identification

Compounds **5** and **6** (1.0 mg each) were each hydrolyzed with 2.0 M HCl (4.0 mL), heated for 1.0 h at 85 °C and extracted with ethyl acetate, and the reaction mixture was concentrated [17]. The residue was dissolved in pyridine (1 mL) and reacted with ʟ-cysteine methyl ester (4.0 mg) for 1.0 h at 60 °C, and then *o*-tolyl isothiocyanate (10 μL) was added to the mixture and stirred at 60 °C for another 1.0 h. The derivatives were analyzed by HPLC and detected at 250nm [18]. Mobile phase: MeCN-H$_2$O (25:75), flow rate: 1.0 mL/min, t$_R$ = 15.54 min (ʟ-glucose), t$_R$ = 16.98 min (ᴅ-glucose), and the migration time of the derivatives of **5** and **6** was also 16.98 min, which revealed the sugar moiety in compounds **5** and **6** was ᴅ-glucose. The ᴅ-glucose and ʟ-glucose as reference samples were also derivatized and analyzed applying the same procedures mentioned above.

3.5. Cell Culture

The murine RAW 264.7 macrophage cells were obtained from Cell Bank of the Shanghai Institute of Cell Biology and Biochemistry, Chinese Academy of Sciences (Shanghai, China). The cells were cultured in Dulbecco's modified Eagle's medium containing 10% fetal bovine serum and penicillin-streptomycin (100 U/mL) at 37 °C with 5% CO$_2$.

3.6. Cell Viability Assay

An MTT assay was used to evaluate RAW 264.7 cell viability as previously described [34]. The mitochondrial-dependent reduction of 3-(4,5-dimethylthizaol-2yl)-2,5-diphenyl tetrazolium bromide (MTT) to formazan was used to measure cell respiration as an indicator of cell viability [35]. Briefly, after 24 h incubation with or without compounds (6.25–100 μM), an MTT solution (final concentration 5 mg/mL) was added and the cells were incubated for another 2.5 h at 37 °C. After removing the supernatant, 150 μL of DMSO was added to the cells to dissolve the formazan. The absorbance of each group was measured by using a microplate reader at a wavelength of 490 nm. Results are expressed as a percentage of viable cells when compared with the control group. The viability of RAW 264.7 cells of the control group (with 0.1%DMSO only) is defined as 100%.

3.7. Measurement of NO Release

The accumulated nitrite in the supernatant was evaluated using the Griess reagent [36,37] (Beyotime, Nanjing, China). RAW 264.7 macrophage cells were seeded in 96-well culture plates (5 × 10^4 cells/well) for 24 h. Then, various concentrations of test compounds were added, after 2.5 h incubation, with the presence of 1 μg/mL LPS. 0.1% DMSO and 1 μg/mL LPS without test compounds were added

as model group, only with the presence of 0.1% DMSO and equivalent DMEM as the control group. Twenty hours later, culture supernatant and Griess reagent were mixed and then incubated for 10 min. The optical density of the mixture was read at 540 nm using an automated microplate reader. The NO inhibitory rate was measured in relation to the model group (cells were treated with LPS only). Berberine (purity ≥98%, Yuanye, Shanghai, China) served as the positive control.

Supplementary Materials: Supplementary Materials are available online.

Author Contributions: P.-F.W. and Y.-P.L. performed the experiments, and wrote the first version of the manuscript; L.-Q.D., S.-J.C. and L.-N.W. designed the experiment; L.N.W. approved and revised the submitted manuscript; F.Q. presented the conception of the project, acquired the funding, supervised the execution of the whole project, and drafted and edited the final manuscript.

Conflicts of Interest: The authors declare no conflicts of interest.

Abbreviations

DMEM	dulbecco's modified eagle medium
DMSO	Dimethyl Sulfoxide
HMBC	Heteronuclear Multiple Bonding Correlation
HSQC	Heteronuclear Single Quantum Correlation
MTT	3-(4,5-dimethyl-2-thiazolyl)-2,5-diphenyl-2-H-tetrazolium bromide
NOE	Nuclear Overhauser Enhancement
NOESY	Nuclear Overhauser Enhancement Spectroscopy
RAW	leukemia cellsin mouse macrophage

References

1. Shiao, P.G. *Photocatalogue of Chinese Traditional Medicine*; Taiwan Business Publication Company: Taipei, Taiwan, 1990; Volume 10, p. 86.

2. Hsu, K.J. *Chinese Traditional Medicine*; Chinese Pharmaceutical Science and Technology Publication Company: Beijing, China, 1996; p. 802.

3. Chinese Pharmacopoeia Commission. *Pharmacopoeia of the People's Republic of China*; Chemical Industry Press: Beijing, China, 2015; pp. 305–306.

4. Chen, M.L.; Xian, Y.F.; Ip, S.P.; Tsai, S.H.; Yang, J.Y. Chemical and Biological Differentiation of Cortex Phellodendri Chinensis and Cortex Phellodendri Amurensis. *Planta Med.* **2010**, *76*, 1530–1535. [CrossRef] [PubMed]

5. Wu, T.S.; Hsu, M.Y.; Kuo, P.C.; Sreenivasulu, B.; Damu, A.G.; Su, C.R. Constituents from the leaves of *Phellodendron amurense* var. *wilsonii* and their bioactivity. *J. Nat. Prod.* **2003**, *66*, 1207–1211. [CrossRef] [PubMed]

6. Yan, C.; Zhang, Y.D.; Wang, X.H.; Geng, S.D.; Wang, T.Y.; Sun, M. Tirucallane-type triterpenoids from the fruits of *Phellodendron chinense* Schneid and their cytotoxic activities. *Fitoterapia* **2016**, *113*, 132–138. [CrossRef] [PubMed]

7. Cuéllar, M.J.; Giner, R.M.; Recio, M.C.; Máñez, S.; RíOs, J.L. Topical anti-inflammatory activity of some Asian medicinal plants used in dermatological disorders. *Fitoterapia* **2001**, *72*, 221–229. [CrossRef]

8. Park, S.D.; Lai, Y.S.; Kim, C.H. Immunopontentiating and antitumor activities of the purified polysaccharides from *Phellodendron chinense* SCHNEID. *Life Sci.* **2004**, *75*, 2621–2632. [CrossRef]

9. Ishii, T.; Yanagisawa, M. Synthesis, separation and NMR spectral analysis of methyl apiofuranosides. *Carbohydr. Res.* **1998**, *313*, 189–192. [CrossRef]

10. Ishiia, T.; Ono, H. NMR ctroscopic analysis of the borate diol esters of methyl apiofuranosides. *Carbohydr. Res.* **1999**, *321*, 257–260. [CrossRef]

11. Park, S.; Goo, Y.M.; Na, D.S. Isolation and structure elucidation of a catechin glycoside with phospholipase A2 inhibiting activity from Ulmi cortex. *Bull. Korean Chem. Soc.* **1996**, *17*, 101–103.

12. Angyal, S.J.; Bodkin, C.L.; Mills, J.A.; Pojer, P.M. ChemInform Abstract: Complexes of carbohydrates with metal cations. IX Synthesis of the methyld D-tagatosides, D-psicosides, D-apiosides, and D-erythrosides. *Cheminform* **1977**, *8*, 1259–1268. [CrossRef]

13. Tronchet, J.M.J.; Tronchet, J. 9-(3-C-hydroxymethyl-α-L-threofuranosyl) adenine (9-(β-Dapio-L-furanosyl) adenine). *Carbohydr. Res.* **1974**, *34*, 263–270. [CrossRef]

14. Zhang, N.; Huang, W.X.; Xia, G.Y.; Oppong, M.B.; Ding, L.Q.; Li, P.; Qiu, F. Methods for determination of absolute configuration of monosaccharides. *Chin. Herb. Med.* **2018**, *10*, 14–22. [CrossRef]

15. Mathias, L.; Vieira, I.J.C.; Filho, R.B.; Filho, R.E. A New Isoflavone Glycoside from Dalbergia nigra. *J. Nat. Prod.* **1998**, *61*, 1158–1161. [CrossRef]

16. Zhou, K.L.; Zhao, F.; Liu, Z.H.; Zhuang, Y.L.; Chen, L.X.; Qiu, F. Triterpenoids and Flavonoids from Celery (Apium graveolens). *J. Nat. Prod.* **2009**, *72*, 1563–1567. [CrossRef]

17. Tanaka, T.; Nakashima, T.; Ueda, T. Facile Discrimination of Aldose Enantiomers by Reversed-Phase HPLC. *Chem. Pharm. Bull.* **2007**, *55*, 899–901. [CrossRef]

18. Murata, T.; Endo, Y.; Miyase, T.; Yoshizaki, F. Iridoid glycoside constituents of Stachys lanata. *J. Nat. Prod.* **2008**, *71*, 1768–1770. [CrossRef]

19. Johnsson, P.; Peerlkamp, N. Polymeric fractions containing phenol glucosides in flaxseed. *Food Chem.* **2002**, *6*, 207–212. [CrossRef]

20. Rowe, J.W.; Bower, C.L.; Wagner, E.R. Extractives of jack pine bark: Occurrence of cis- and trans-pinosylvin dimethyl ether and ferulic acid esters. *Phytochemistry* **1969**, *8*, 235–241. [CrossRef]

21. Andrade, P.B.; Leitão, R.; Seabra, R.M. 3,4-Dimethoxycinnamic acid levels as a tool for differentiation of Coffea canephora var. robusta and Coffea arabica. *Food Chem.* **1998**, *61*, 511–514. [CrossRef]

22. Gopalakrishnan, S.; Subbarao, G.V.; Nakahara, K. Nitrification inhibitors from the root tissues of Brachiaria humidicola, a tropical grass. *J. Agric. Food. Chem.* **2007**, *55*, 1385–1388. [CrossRef]

23. Vongvanich, N.; Kittakoop, P.; Charoenchai, P. Antiplasmodial, Antimycobacterial, and Cytotoxic Principles from Camchaya calcarea. *Planta Med.* **2006**, *72*, 1427–1430. [CrossRef]

24. Xiao, H.; Parkin, K.L. Isolation and identification of potential cancer chemopreventive agents from methanolic extracts of green onion (Allium cepa). *Phytochemistry* **2007**, *68*, 1059–1067. [CrossRef]

25. Nakamura, S.; Fujimoto, K.; Matsumoto, T. Acylated sucroses and acylated quinic acids analogs from the flower buds of Prunus mume and their inhibitory effect on melanogenesis. *Phytochemistry* **2013**, *92*, 128–136. [CrossRef]

26. Youn, U.J.; Lee, J.H.; Lee, Y.J. Regulation of the 5-HT3A Receptor-Mediated Current by Alkyl 4-Hydroxybenzoates Isolated from the Seeds of Nelumbo nucifera. *Clin. Biochem.* **2010**, *7*, 2296–2302.

27. Chai, W.M.; Shi, Y.; Feng, H.L. NMR, HPLC-ESI-MS, and MALDI-TOF MS Analysis of Condensed Tannins from Delonix regia (Bojer ex Hook.) Raf. and Their Bioactivities. *J. Agric. Food. Chem.* **2012**, *60*, 5013–5022. [CrossRef] [PubMed]

28. Majumder, P.L.; Banerjee, S.; Sen, S. Three stilbenoids from the orchid Agrostophyllum callosum. *Phytochemistry* **1996**, *42*, 847–852. [CrossRef]

29. David, A.G.; Timothy, R.B. Molecular biology of nitric oxide synthases. *Cancer Metast. Rev.* **1998**, *17*, 7–23.

30. Beckman, J.S.; Koppenol, W.H. Nitric oxide, superoxide, and peroxynitrite: the good, the bad, and ugly. *Am. J. Physiol.* **1996**, 1424–1437. [CrossRef]

31. Bungorn, S.; Jintana, J.; Nawarat, W.; Doosadee, H. Anti-inflammatory effect of Streblus asperleaf extract in rats and its modulationon inflammation-associated genes expression in RAW 264.7 macrophage cells. *J. Ethnopharmacol.* **2009**, *124*, 566–570.

32. Guzik, T.J.; Korbut, R.; Adamek, G.T. Nitric oxide and superoxide in inflammation and immune regulation. *J. Physiol. Pharmacol.* **2003**, *54*, 469.

33. Naohiro, O.; Tomofumi, S.; Yuji, N.; Noriyasu, H.; Fumiyuki, K. Quantitative analysis of the anti-inflammatory activity of orengedokuto II: berberine is responsible for the inhibition of NO production. *J. Nat. Med.* **2018**, *72*, 706–714.

34. Sun, L.D.; Wang, F.; Dai, F.; Wang, Y.H.; Lin, D.; Zhou, B. Development and mechanism investigation of a new piperlongumine derivative as a potent anti-inflammatory agent. *Biochem. Pharmacol.* **2015**, *95*, 156–169. [CrossRef] [PubMed]

35. Xue, G.M.; Li, X.Q.; Chen, C. Highly Oxidized Guaianolide Sesquiterpenoids with Potential Antiinflammatory Activity from Chrysanthemum indicum. *J. Nat. Prod.* **2018**, *81*, 378–386. [CrossRef]

36. Zhao, F.; Wang, L.; Liu, K. In vitro anti-inflammatory effects of arctigenin, a lignan from Arctium lappa L. through inhibition on iNOS pathway. *J. Ethnopharmacology.* **2009**, *122*, 457–462. [CrossRef] [PubMed]

37. Choi, Y.Y.; Kim, M.H.; Han, J.M.; Hong, J.K.; Lee, T.H.; Kim, S.H. The anti-inflammatory potential of Cortex Phellodendron in vivo and in vitro: down-regulation of NO and iNOS through suppression of NF-κB and MAPK activation. *Int. J. Immunopharmacol.* **2014**, *19*, 214–220. [CrossRef] [PubMed]

Sample Availability: Samples of the compounds are not available from the authors.